Effective spring boundary conditions for a damaged interface between dissimilar media in three-dimensional case

Effective spring boundary conditions for a damaged interface between dissimilar media in three-dimensional case

Mikhail V. Golub[a,*], Olga V. Doroshenko[a], Anders Boström[b]

[a]*Institute for Mathematics, Mechanics and Informatics, Kuban State University, Krasnodar, 350040 Russia*
[b]*Department of Applied Mechanics, Chalmers University of Technology, SE-412 96 Göteborg, Sweden*

Abstract

Elastic waves in the presence of a damaged interface between two dissimilar elastic media is investigated in the three-dimensional case. The damaged is modelled as a stochastic distribution of equally sized circular cracks which is transformed into a spring boundary condition. First the scattering by a single circular interface crack between two dissimilar half-spaces is investigated and solved explicitly for normally incident waves in the low frequency limit. The transmission by a distribution of cracks is then determined and is transformed into a spring boundary condition, where effective spring stiffnesses are expressed in terms of elastic moduli and damage parameters. A comparison with previous results for a periodic distribution of cracks shows good agreement.

Keywords: imperfect contact, delamination, elastic waves, spring

*Corresponding author
Email addresses: m_golub@inbox.ru (Mikhail V. Golub), oldorosh@mail.ru (Olga V. Doroshenko), anders.bostrom@chalmers.se (Anders Boström)

boundary condition, spring stiffness, crack, diffraction, dissimilar materials

1. Introduction

Elastic wave scattering by damage and delaminations is of considerable importance for ultrasonic non-destructive evaluation and structural health monitoring, where ultrasound is widely used to detect interfacial damage. Ultrasound methods should distinguish between an open crack, where all the faces are stress-free, and a delamination. A delamination can be more complex than an open crack: faces may interact or consist of multiple microcracks, especially at adhesive bonds. Identification of damaged interfaces or zones of non-perfect contact between materials is more complicated than identification of macrocracks. An imperfection can be simulated as a set or multiple cracks (Achenbach, 1989; Achenbach and Zhang, 1990) or as a deviation from perfect contact (Tattersall, 1973; Baik and Thompson, 1984), and this leads to a modification of the continuous boundary conditions at the interface. Although the approaches are technically different, they lead to similar results related to wave propagation in composites with damaged interfaces (Baik and Thompson, 1984; Achenbach, 1989; Golub and Boström, 2011; Kvasha et al., 2011).

It is natural to introduce a distribution of springs at the debonded interface (spring boundary conditions) in order to simulate it. Compared to multiple cracks, spring boundary conditions are simpler and more efficient. Thus, spring boundary conditions can be used for identification of multiple cracks (Shifrin, 2015). Tattersall (1973) showed experimentally that an imperfect contact can be investigated with elastic waves. This idea of using

ultrasound in order to test adhesive bonds or debonded interfaces is applied by, e.g., Alers and Graham (1975), who demonstrated the applicability of spring boundary conditions for the estimation of adhesive bonds. The spring boundary conditions at the interface with normal $\boldsymbol{n}$ demand that the normal and tangential components of stress σ are continuous while the jump in the displacement vector is proportional to the stress:

$$\sigma_{ik}^{1} \cdot n_k = \sigma_{ik}^{2} \cdot n_k = \kappa_{ik} \left(u_k^2 - u_k^1 \right). \tag{1}$$

Here κ_{ik} is in general a three-by-three matrix and the upper indices number the contacting media.

Other approaches such as introducing a set of cracks or replacing a damaged layer by a thin layer have also been applied and compared with the spring model (Baik and Thompson, 1984; Sotiropoulos and Achenbach, 1988; Kachanov, 1994, etc.). Many studies exploiting distributed springs have been applied to simulate ultrasound interaction with planar damaged interfaces with different structures. Many of them (Baik and Thompson, 1984; Margetan et al., 1988; Boström and Wickham, 1991; Lavrentyev and Rokhlin, 1994; Pecorari, 2008; Boström and Golub, 2009; Lekesiz et al., 2013a) derived estimations for the distributed spring stiffnesses or applied these models in experimental work (Lavrentyev and Rokhlin, 1998; Leiderman and Castello, 2014). These derivations are often based on the idea of substitution of an array of planar cracks by distributed springs at the damaged interface. This substitution should lead to the same wavefields in the far-field zone from the interface. It should be mentioned that normal and transverse spring stiffnesses are equal in the case of in-plane motion (Lekesiz et al., 2011; Golub and Boström, 2011), while they differ in the three-dimensional case (Lekesiz

et al., 2013a). Baik and Thompson (1984) used a quasi-static approximation for plane P-waves and obtained the expression for effective normal spring stiffness for identical materials. Margetan et al. (1988) extended this approach and estimated the transverse component of the spring stiffness for identical media, Lavrentyev and Rokhlin (1994) derived the stiffnesses for the case of dissimilar materials at the imperfect contact zone. An effective spring stiffness approximation was proposed for a planar periodic array of collinear cracks (Lekesiz et al., 2011) and a hexagonal array of coplanar penny shaped cracks located at the interface between two dissimilar solids (Lekesiz et al., 2013a).

The present paper is an extension of previous work on distributions of strip-like cracks between dissimilar media (Boström and Golub, 2009; Golub, 2010; Golub and Boström, 2011; Kvasha et al., 2011) and the study of Boström and Wickham (1991), where a distribution of circular contacts between two identical half-spaces were considered. The aim of this study is to obtain expressions for the spring boundary conditions in three dimensions describing wave propagation through a damaged interface between dissimilar isotropic media in terms of elastic moduli and damage parameters. First, an integral equation for a circular interface crack is derived following Krenk and Schmidt (1982) combined with an integral equation technique (Glushkov and Glushkova, 2001; Glushkov et al., 2002). The scheme used by Boström and Wickham (1991) is applied in order to obtain the total transmission coefficients for a distribution of cracks using a reciprocal theorem and ensemble averaging. In order to construct analytical formulae, an asymptotic low frequency solution for a single circular crack between dissimilar half-spaces is

derived, see Ohyoshi (1973); Vatulyan and Yavruyan (2006). Then the reflection and transmission coefficients for normal incidence of a plane P-wave and S-wave for a random distribution of equally sized circular cracks at the interface between two half-spaces are calculated. The diagonal components of the spring stiffness matrix are derived from the equality of the transmission coefficients for the spring model and the damaged interface.

2. Single interface crack

In this section the scattering of time harmonic waves by an open, circular crack at the interface between two dissimilar elastic isotropic half-spaces is investigated. Cartesian (x_1, x_2, x_3) and cylindrical (r, θ, z) coordinate systems are used in the following, both are centred at the circular crack occupying the domain $\Omega = \{r \leq a, z = 0\}$ as depicted in Figure 1. The displacement vector is denoted $\boldsymbol{u}^j = u_i^j = \{u_1^j, u_2^j, u_3^j\}$, where superscript $j = 1$ corresponds to the lower half-space ($x_3 < 0$) and $j = 2$ to the upper one ($x_3 > 0$). The material properties are determined by the Lamé constants λ_j and μ_j and densities ρ_j. The wave numbers $k_{ij} = \omega / v_{ij}$ at the angular frequency ω are expressed via the longitudinal or P wave velocity v_{1j} and the transverse or S wave velocity v_{2j}:

$$v_{nj} = \sqrt{c_{nj}/\rho_j}, \quad c_{1j} = \lambda_j + 2\mu_j, \quad c_{2j} = \mu_j.$$

Harmonic motion in isotropic media is governed by the Lamé equation

$$\sum_{i=1}^{3} \frac{\partial \sigma_{ik}^j}{\partial x_k} + \rho^j \omega^2 u_i^j = 0, \qquad j = 1, 2. \tag{2}$$

The stress tensor components are given by Hooke's law:

$$\sigma_{ik}^j = \lambda_j \left(\frac{\partial u_1^j}{\partial x_1} + \frac{\partial u_2^j}{\partial x_2} + \frac{\partial u_3^j}{\partial x_3} \right) \delta_{ik} + \mu_j \left(\frac{\partial u_i^j}{\partial x_k} + \frac{\partial u_k^j}{\partial x_i} \right).$$

where δ_{ik} is the Kronecker delta.

The total field in the two half-spaces with a circular interface crack is a sum of an incident field in the absence of the crack $\boldsymbol{u}^{\rm in}$ and a scattered field $\boldsymbol{u}^{\rm sc}$ due to the crack. For the purposes of this study the incident field $\boldsymbol{u}^{\rm in}$ is taken as a plane wave propagating along the x_3 axis in the lower half-space plus the corresponding reflected and transmitted waves:

$$\boldsymbol{u}_s^{\rm in}(x_1,x_2,x_3) = \begin{cases} \boldsymbol{p}_s \left({\rm e}^{{\rm i}k_{1s}x_3} + R_s^- {\rm e}^{-{\rm i}k_{1s}x_3} \right), & x_3 < 0, \\ \boldsymbol{p}_s T_s^- {\rm e}^{{\rm i}k_{2s}x_3}, & x_3 > 0, \end{cases} , \tag{3}$$

The index s here takes the value $s = 1$ for an incoming P wave and $s = 2$ for an incoming S wave. The amplitude reflection and transmission coefficients are

$$R_s^- = \frac{c_{1s}k_{1s} - c_{2s}k_{2s}}{c_{1s}k_{1s} + c_{2s}k_{2s}}, \qquad T_s^- = \frac{2c_{1s}k_{1s}}{c_{1s}k_{1s} + c_{2s}k_{2s}}, \quad s = 1, 2. \tag{4}$$

The polarization vector $\boldsymbol{p}_s$ describing the type of incident plane wave is for the P wave $\boldsymbol{p}_1 = \{0, 0, 1\}$ and for the S wave $\boldsymbol{p}_2 = \{1, 0, 0\}$.

The wave scattered by an open crack $\boldsymbol{u}^{\rm sc}$ has continuous normal and tangential stresses $\boldsymbol{\tau}^{\rm sc} = \{\sigma_{13}, \sigma_{23}, \sigma_{33}\}$ at the interface of the crack $x_3 = 0$, whereas the displacement field $\boldsymbol{u}^{\rm sc}$ has a discontinuity at $r \leq a$ so the boundary conditions for the scattered field are:

$$\begin{cases} \boldsymbol{u}^{1,{\rm sc}}(r,\theta,0) = \boldsymbol{u}^{2,{\rm sc}}(r,\theta,0), & r > a, \\ \boldsymbol{\tau}^{1,{\rm sc}}(r,\theta,0) = \boldsymbol{\tau}^{2,{\rm sc}}(r,\theta,0), & r > a, \\ \boldsymbol{\tau}^{1,{\rm sc}}(r,\theta,0) = \boldsymbol{\tau}^{2,{\rm sc}}(r,\theta,0) = -\boldsymbol{\tau}_s^{1,{\rm in}}(r,\theta,0), & r \leq a. \end{cases} \tag{5}$$

In addition the scattered field must be outgoing at infinity.

The scheme used by Krenk and Schmidt (1982) for a circular crack in an isotropic space is now followed. Thus cylindrical coordinates are used and

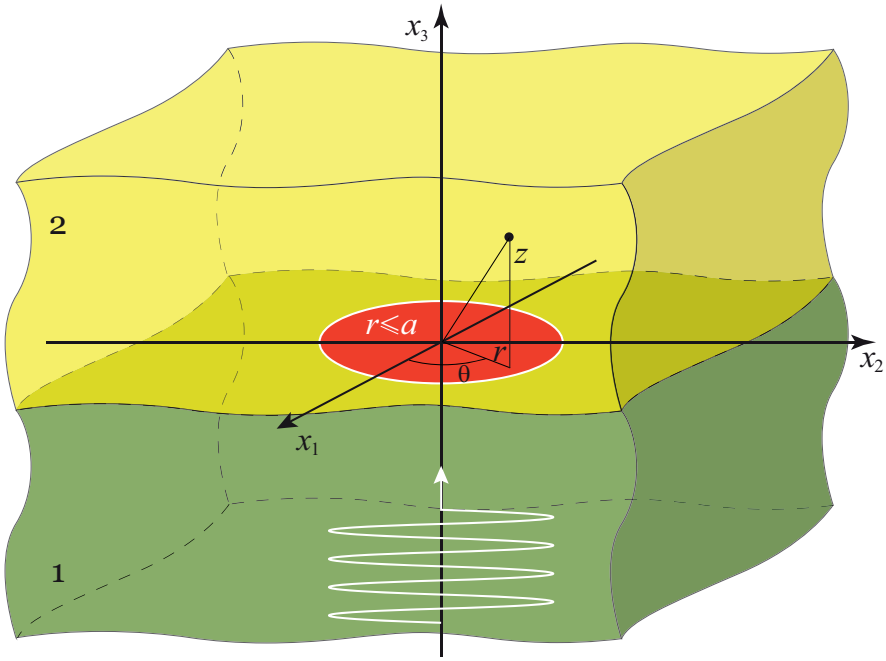

Figure 1: Geometry of the problem for a single interface crack.

the cylindrical displacement components are written

$$u_r = \frac{\partial \psi_3}{\partial r} + \frac{\partial^2 \psi_2}{\partial r \partial z} + \frac{1}{r}\frac{\partial \psi_1}{\partial \theta}, \quad u_\theta = \frac{1}{r}\frac{\partial \psi_3}{\partial \theta} + \frac{1}{r}\frac{\partial^2 \psi_2}{\partial \theta \partial z} - \frac{\partial \psi_1}{\partial r},$$

$$u_z = \frac{\partial \psi_3}{\partial z} - \left(\nabla^2 - \frac{\partial^2}{\partial z^2}\right)\psi_2,$$

in terms of potentials ψ_i. The index j denoting the half-space is suppressed on the potentials here and in the following. The potentials in media denoted by index $j = 1, 2$ must satisfy Helmholtz equations

$$\nabla^2 \psi_3 + k_{1j}^2 \psi_3 = 0, \qquad \nabla^2 \psi_i + k_{2j}^2 \psi_i = 0, \quad i = 1, 2.$$

In order to construct solutions in cylindrical coordinates the wavefields are expanded into Fourier series in terms of $\cos m\theta$ and $\sin m\theta$ over the angular

coordinate θ. The potentials for the scattered field have similar representations, where the potential ψ_1^m differs by a sign (Krenk and Schmidt, 1982; Boström and Peterson, 1989)

$$\psi_1(r,\theta,z) = \sum_{m=0}^{\infty} \psi_1^{1m}(r,z)\sin m\theta - \sum_{m=0}^{\infty} \psi_1^{2m}(r,z)\cos m\theta,$$

$$\psi_i(r,\theta,z) = \sum_{m=0}^{\infty} \psi_i^{1m}(r,z)\cos m\theta + \sum_{m=0}^{\infty} \psi_i^{2m}(r,z)\sin m\theta, \quad i = 2,3.$$

Expressions for the components of the displacement vector $\boldsymbol{v} = \{u_r, u_\theta, u_z\}$ and stress vector have the same form:

$$\boldsymbol{v}(r,\theta,z) = \sum_{m=0}^{\infty} \Big(\boldsymbol{\chi}^{1m}(\theta)\boldsymbol{v}^{1m}(r,z) + \boldsymbol{\chi}^{2m}(\theta)\boldsymbol{v}^{2m}(r,z) \Big),$$

$$\boldsymbol{\tau}(r,\theta,z) = \sum_{m=0}^{\infty} \Big(\boldsymbol{\chi}^{1m}(\theta)\boldsymbol{\tau}^{1m}(r,z) + \boldsymbol{\chi}^{2m}(\theta)\boldsymbol{\tau}^{2m}(r,z) \Big),$$

where

$$\boldsymbol{\chi}^{1m}(\theta) = \mathrm{diag}\big(\cos(m\theta), \sin(m\theta), \cos(m\theta)\big),$$

$$\boldsymbol{\chi}^{2m}(\theta) = \mathrm{diag}\big(\sin(m\theta), -\cos(m\theta), \sin(m\theta)\big).$$

It is natural to represent the functions $\psi_i^{nm}(r,z)$ as the Hankel transform of $\Psi_i^m(\alpha,z)$ over the radial coordinate r

$$\psi_i^{nm}(r,z) = \int_0^{\infty} \Psi_i^{nm}(\alpha,z) J_m(\alpha r)\alpha \mathrm{d}\alpha.$$

It is also convenient to follow (Krenk and Schmidt, 1982; Boström and Peterson, 1989) and to use rearranged displacement

$$\boldsymbol{w}^{nm} = \{u_r^{nm} + u_\theta^{nm}, u_r^{nm} - u_\theta^{nm}, u_z^{nm}\}$$

and stress vectors

$$\widehat{\boldsymbol{\tau}}^{nm} = \{\tau_{rz}^{nm} + \tau_{\theta z}^{nm}, \tau_{rz}^{nm} - \tau_{\theta z}^{nm}, \tau_{zz}^{nm}\}\,. \tag{6}$$

Here the Fourier components are expressed in terms of the Hankel transform, see (Glushkov and Glushkova, 2001; Glushkov et al., 2002) for more details

$$\boldsymbol{w}^{\mathrm{sc},nm}(r,z) = \begin{cases} \boldsymbol{w}_1^{\mathrm{sc},nm}(r,z) = \int\limits_0^\infty \mathbf{J}^m(\alpha r)\mathbf{K}_1(\alpha,z)\boldsymbol{Q}^{nm}(\alpha)\alpha\,\mathrm{d}\alpha, & z<0 \\ \boldsymbol{w}_2^{\mathrm{sc},nm}(r,z) = \int\limits_0^\infty \mathbf{J}^m(\alpha r)\mathbf{K}_2(\alpha,z)\boldsymbol{Q}^{nm}(\alpha)\alpha\,\mathrm{d}\alpha, & z>0 \end{cases} \tag{7}$$

To obtain this representation the continuity of the components $q_i^{nm}(r)$ of the unknown traction vector

$$\widehat{\boldsymbol{\tau}}^{\mathrm{sc}}(r,\theta) = \boldsymbol{q}(r,\theta) = \sum_{m=0}^{\infty}\sum_{n=1}^{2}\boldsymbol{\chi}^{nm}(\theta)\boldsymbol{q}^{nm}(r)$$

over the whole interface has been used in the form of the Hankel transform:

$$\boldsymbol{Q}^{nm}(\alpha) = \int\limits_0^\infty \mathbf{J}^m(\alpha r)\boldsymbol{q}^{nm}(r)r\,\mathrm{d}r.$$

In the integral representation (7) the Hankel transform of Green's matrices is

$$\mathbf{K}_j(\alpha,z) = \begin{pmatrix} \frac{1}{2}\left[M_j(\alpha,z)+N_j(\alpha,z)\right] & -\frac{1}{2}\left[M_j(\alpha,z)-N_j(\alpha,z)\right] & P_j(\alpha,z) \\ -\frac{1}{2}\left[M_j(\alpha,z)-N_j(\alpha,z)\right] & \frac{1}{2}\left[M_j(\alpha,z)+N_j(\alpha,z)\right] & -P_j(\alpha,z) \\ -\frac{1}{2}S_j(\alpha,z) & \frac{1}{2}S_j(\alpha,z) & R_j(\alpha,z) \end{pmatrix},$$

and the matrix composed of Bessel functions is

$$\mathbf{J}^m(\alpha r) = \begin{pmatrix} J_{m+1}(\alpha r) & 0 & 0 \\ 0 & J_{m-1}(\alpha r) & 0) \\ 0 & 0 & J_m(\alpha r) \end{pmatrix}.$$

The shifts in orders of the Bessel functions in $\mathbf{J}^m$ occur due to the use of the displacement vector $\boldsymbol{w}^{nm}$ instead of $\boldsymbol{v}$. The components of the Hankel transform of the Green's matrices $\mathbf{K}_j$ are expressed via the same functions as in (Glushkov et al., 2002)

$$\begin{aligned} M_j(\alpha,z) &= (-1)^{j+1}\frac{\gamma_{2j}}{\Delta_j}\left[\eta_j \mathrm{e}^{-\gamma_{2j}|z|} - 2\alpha^2 \mathrm{e}^{-\gamma_{1j}|z|}\right], \\ R_j(\alpha,z) &= (-1)^{j}\frac{\gamma_{1j}}{\Delta_j}\left[2\alpha^2 \mathrm{e}^{-\gamma_{2j}|z|} - \eta_j \mathrm{e}^{-\gamma_{1j}|z|}\right], \\ P_j(\alpha,z) &= \frac{\alpha}{\Delta_j}\left[2\gamma_{1j}\gamma_{2j} \mathrm{e}^{-\gamma_{2j}|z|} - \eta_j \mathrm{e}^{-\gamma_{1j}|z|}\right], \\ S_j(\alpha,z) &= \frac{\alpha}{\Delta_j}\left[\eta_j \mathrm{e}^{-\gamma_{2j}|z|} - 2\gamma_{1j}\gamma_{2j} \mathrm{e}^{-\gamma_{1j}|z|}\right], \\ N_j(\alpha,z) &= (-1)^{j+1}\frac{\mathrm{e}^{-\gamma_{2j}|z|}}{\mu_j\gamma_{2j}}, \\ \Delta_j = \mu_j[\eta_j^2 - 4\alpha^2\gamma_{1j}\gamma_{2j}], &\qquad \eta_j = (2\alpha^2 - k_{2j}^2). \end{aligned} \tag{8}$$

The branches of the square roots $\gamma_{nj} = \sqrt{\alpha^2 - k_{nj}^2}$ are fixed by the conditions $\operatorname{Re}\gamma_{nj} \geq 0$ and $\operatorname{Im}\gamma_{nj} \leq 0$ for $\alpha \in (-\infty, \infty)$.

It is convenient to introduce the crack opening displacement (COD) as the primary unknown (for which an integral equation is going to be formulated)

$$\Delta\boldsymbol{v}(r,\theta) = \boldsymbol{v}_1^{\mathrm{sc}}(r,\theta,0) - \boldsymbol{v}_2^{\mathrm{sc}}(r,\theta,0) = \sum_{n=1}^{2}\sum_{m=0}^{\infty}\boldsymbol{\chi}^{nm}(\theta)\Delta\boldsymbol{v}^{nm}(r) \tag{9}$$

The combinations $\Delta\boldsymbol{w}^{nm}$ of the components of $\Delta\boldsymbol{v}^{nm}$ are expanded into a series of the associated Legendre polynomials P_j^m of the first kind (Krenk and Schmidt, 1982; Kundu and Boström, 1991):

$$\Delta w_k(r,\theta) = \sum_{n=1}^{2}\sum_{m=0}^{\infty}\sum_{t=0}^{\infty}\beta_{kt}^{nm}\phi_{kt}^m(r)\chi^{nm}(\theta) \tag{10}$$

$$\phi_{1t}^m(r) = \frac{P_{m+2t+2}^{m+1}\left(\sqrt{1-r^2/a^2}\right)}{P_{m+2t+2}^{m+2}(0)}, \quad \phi_{2t}^m(r) = \frac{P_{m+2t}^{m-1}\left(\sqrt{1-r^2/a^2}\right)}{P_{m+2t}^{m}(0)},$$

$$\phi_{3t}^m(r) = \frac{P_{m+2t+1}^m\left(\sqrt{1-r^2/a^2}\right)}{P_{m+2t+1}^{m+1}(0)}.$$

This expansion has the correct behaviour as r approaches zero and it has a square root behaviour at the crack edge, but it does not have the (somewhat unphysical) oscillations that are known to exist at a crack edge between two dissimilar media (Srivastava et al., 1979). The Hankel transform of the basis functions can be calculated in terms of Bessel functions

$$\Phi_{3t}^m(\alpha a) = \int_0^a \phi_{3t}^m(r) J_m(\alpha r) r \mathrm{d}r = \int_0^a \frac{P_{m+2t+1}^m\left(\sqrt{1-r^2/a^2}\right)}{P_{m+2t+1}^{m+1}(0)} J_m(\alpha r) r \,\mathrm{d}r =$$

$$(-1)^t \sqrt{\frac{\pi a}{2}} \frac{J_{m+2t+1+3/2}(\alpha a)}{\alpha^{3/2}}$$

$$\Phi_{kt}^m(\alpha a) = \int_0^a \phi_{kt}^m(r) J_{m+1}(\alpha r) r \mathrm{d}r = (-1)^t \sqrt{\frac{\pi a}{2}} \frac{J_{m+2t+9/2-2k}(\alpha a)}{\alpha^{3/2}}, \quad k = 1, 2.$$

The basis functions should be defined carefully for $m = 0$, in this case $\phi_{2t}^0(r) = \phi_{1t}^0(r)$ and correspondingly $\Phi_{2t}^0(\alpha a) = \int_0^a \phi_{1t}^0(r) J_{-1}(\alpha r) r \mathrm{d}r = -\Phi_{1t}^0(\alpha a)$.

Using the continuity of the displacement between the two half-spaces outside the crack it is straightforward to express the unknown Hankel transform of the interfacial traction

$$\boldsymbol{Q}^{nm}(\alpha) = \mathbf{L}(\alpha) \Delta \boldsymbol{W}^{nm}(\alpha),$$

$$\mathbf{L}(\alpha) = \left[\mathbf{K}_2(\alpha, 0) - \mathbf{K}_1(\alpha, 0)\right]^{-1}, \quad n = 1, 2.$$

in terms of the crack opening displacement

$$\Delta \boldsymbol{W}^{nm}(\alpha) = \int_0^\infty \mathbf{J}^m(\alpha r) \Delta \boldsymbol{w}^{nm}(r) r \,\mathrm{d}r.$$

For this purpose the integral representation (7) and the inverse Hankel transform are used. The matrix $\mathbf{L}$ becomes

$$\mathbf{L}(\alpha) = \begin{pmatrix} \frac{1}{2}\left[M_0(\alpha) + N_0(\alpha)\right] & -\frac{1}{2}\left[M_0(\alpha) - N_0(\alpha)\right] & P_0(\alpha) \\ -\frac{1}{2}\left[M_0(\alpha) - N_0(\alpha)\right] & \frac{1}{2}\left[M_0(\alpha) + N_0(\alpha)\right] & -P_0(\alpha) \\ -\frac{1}{2}S_0(\alpha) & \frac{1}{2}S_0(\alpha) & R_0(\alpha) \end{pmatrix}.$$

Here the elements can be expressed in analytic form via

$$M_0 = \frac{\widetilde{R}}{\widetilde{M}\widetilde{R} + \widetilde{P}\widetilde{S}}, \quad N_0 = \frac{1}{\widetilde{N}}, \quad P_0 = \frac{-\widetilde{P}}{\widetilde{M}\widetilde{R} + \widetilde{P}\widetilde{S}},$$

$$R_0 = \frac{\widetilde{M}}{\widetilde{M}\widetilde{R} + \widetilde{P}\widetilde{S}}, \quad S_0 = \frac{-\widetilde{S}}{\widetilde{M}\widetilde{R} + \widetilde{P}\widetilde{S}}.$$

The functions with a tilde denote the difference between the corresponding functions (8) without a tilde in the lower and upper half-spaces at $x_3 = 0$, e.g. $\widetilde{M}(\alpha) = M_2(\alpha, 0) - M_1(\alpha, 0)$. These functions become

$$\widetilde{M}(\alpha) = \frac{\gamma_{21}k_{21}^2}{\Delta_1} + \frac{\gamma_{22}k_{22}^2}{\Delta_2}, \quad \widetilde{R}(\alpha) = \frac{\gamma_{11}k_{21}^2}{\Delta_1} + \frac{\gamma_{12}k_{22}^2}{\Delta_2},$$

$$\widetilde{P}(\alpha) = -\widetilde{S}(\alpha) = \alpha\left(-\frac{\gamma_{11}\gamma_{21} - \alpha^2 + k_{21}^2/2}{2\Delta_1} + \frac{\gamma_{12}\gamma_{22} - \alpha^2 + k_{22}^2/2}{2\Delta_2}\right),$$

$$\widetilde{N}(\alpha) = -\frac{\mu_1\gamma_{21} + \mu_2\gamma_{22}}{\mu_1\mu_2\gamma_{21}\gamma_{22}}.$$

To use the inhomogeneous boundary condition at the crack surface (5) the traction of the incoming wave combined according to (6) is also expanded in a Fourier series

$$\widehat{\boldsymbol{\tau}}_s^{\text{in}}(r, \theta, z) = \sum_{n=1}^{2}\sum_{m=0}^{\infty} \boldsymbol{\chi}^{nm}(\theta)\widehat{\boldsymbol{\tau}}_s^{\text{in},nm}(r, z).$$

For the P wave incidence the traction components are

$$\widehat{\boldsymbol{\tau}}_1^{\text{in},nm} = f_1 \begin{cases} (0,0,1), & n = 1, m = 0 \\ (0,0,0), & \text{otherwise} \end{cases},$$

and for SV wave incidence they are

$$\widetilde{\boldsymbol{\tau}}_2^{\mathrm{in},nm} = f_2 \begin{cases} (0,2,0), & n=1, m=1 \\ (0,0,0), & \text{otherwise} \end{cases},$$

$$f_s = \frac{2\mathrm{i}c_{1s}k_{1s}c_{2s}k_{2s}}{c_{1s}k_{1s}+c_{2s}k_{2s}}.$$

The inhomogeneous boundary condition at the crack surface (5) then gives

$$\sum_{n=1}^{2}\sum_{m=0}^{\infty}\boldsymbol{\chi}^{nm}(\theta)\left[\int_0^{\infty}\mathbf{J}^m(\alpha r)\boldsymbol{Q}^{nm}(\alpha)\alpha\mathrm{d}\alpha + \widehat{\boldsymbol{\tau}}^{\mathrm{in},nm}(r,0)\right] = 0.$$

Substitution of the crack opening displacement finally leads to the following integral equation for the unknowns $\Delta\boldsymbol{W}^{nm}$

$$\int_0^{\infty}\mathbf{J}^m(\alpha r)\mathbf{L}(\alpha)\Delta\boldsymbol{W}^{nm}(\alpha)\alpha\mathrm{d}\alpha = -\widehat{\boldsymbol{\tau}}_s^{\mathrm{in},nm}(r). \tag{11}$$

Applying the Galerkine scheme gives the discretized form of the integral equation (11) (keeping N_t+1 terms)

$$\sum_{t=0}^{N_t}\mathbf{A}_{tt'}^m\boldsymbol{\beta}_t^{nm} = -\boldsymbol{g}_{t's}^{nm}, \quad t'=0,\dots N_t \tag{12}$$

where the left-hand side matrix is composed of 3 by 3 blocks

$$\mathbf{A}_{tt'}^m = \int_0^{\infty}\boldsymbol{\Phi}_{t'}^m(\alpha)\mathbf{L}(\alpha)\boldsymbol{\Phi}_t^m(\alpha)\alpha\,\mathrm{d}\alpha, \qquad g_{it's}^{nm} = \int_0^{a}\widehat{\tau}_{is}^{\mathrm{in},nm}(r,0)\phi_{it'}^m(r)r\,\mathrm{d}r,$$

constructed via the matrices $\boldsymbol{\Phi}_{t'}^m = \mathrm{diag}\,(\Phi_{1t'}^m, \Phi_{2t'}^m, \Phi_{3t'}^m)$.

The α integral in $\mathbf{A}_{tt'}^m$ is slowly convergent so the asymptotic behaviour for large arguments is now investigated. For $\alpha\to\infty$ it is possible to expand $\mathbf{L}(\alpha)$ as follows

$$\mathbf{L}(\alpha) = \alpha\,\mathbf{L}_{\mathrm{as}} + \widetilde{\mathbf{L}}(\alpha),$$

where $\widetilde{\mathbf{L}}(\alpha) \sim O(\alpha^{-1})$ at $\alpha \to \infty$. To obtain this the square roots are first expanded

$$\gamma_{nj} = \alpha \left(1 - \frac{k_{nj}^2}{2\alpha^2}\right) + O(1). \tag{13}$$

Then all the functions including γ_{nj} can be also expanded, e.g.

$$\Delta_j \approx 2\mu_j \alpha^2 (k_{1j}^2 - k_{2j}^2) + O(1).$$

Employing these approximations into all the functions involved in the Green's matrix $\mathbf{K}(\alpha, z = 0)$ construction gives

$$\widetilde{M}(\alpha) \approx -\frac{1}{\alpha} m_1, \quad \widetilde{N}(\alpha) \approx -\frac{1}{\alpha} m_2, \quad \widetilde{R}(\alpha) \approx -\frac{1}{\alpha} m_1, \quad \widetilde{P}(\alpha) = -\widetilde{S}(\alpha) \approx \frac{1}{\alpha} m_3,$$

where

$$\begin{gathered} m_1 = \frac{1}{2}\left(\frac{\lambda_1 + 2\mu_1}{\mu_1(\lambda_1 + \mu_1)} + \frac{\lambda_2 + 2\mu_2}{\mu_2(\lambda_2 + \mu_2)}\right), \quad m_2 = \left(\frac{1}{\mu_1} + \frac{1}{\mu_2}\right), \\ m_3 = -\frac{1}{2}\left(\frac{1}{\lambda_1 + \mu_1} - \frac{1}{\lambda_2 + \mu_2}\right). \end{gathered} \tag{14}$$

Substitution of these asymptotic forms into $\mathbf{L}(\alpha)$ gives the final asymptotic representation of the kernel of the integral equation (11)

$$\mathbf{L}_{\text{as}} = \frac{1}{2m_2(m_3^2 - m_1^2)} \begin{pmatrix} m_1^2 + m_1 m_2 - m_3^2 & m_1^2 - m_1 m_2 - m_3^2 & 2m_2 m_3 \\ m_1^2 - m_1 m_2 - m_3^2 & m_1^2 + m_1 m_2 - m_3^2 & -2m_2 m_3 \\ -m_2 m_3 & m_2 m_3 & 2m_1 m_2 \end{pmatrix}.$$

This well-known trick makes it possible to compute the matrix $\mathbf{A}_{tt'}^m$ with a reasonable convergence in the following way

$$\mathbf{A}_{tt'}^m = \widetilde{\mathbf{A}}_{tt'}^m + \int_0^\infty \mathbf{\Phi}_{t'}^m(\alpha) \widetilde{\mathbf{L}}(\alpha) \mathbf{\Phi}_t^m(\alpha)\, \mathrm{d}\alpha, \tag{15}$$

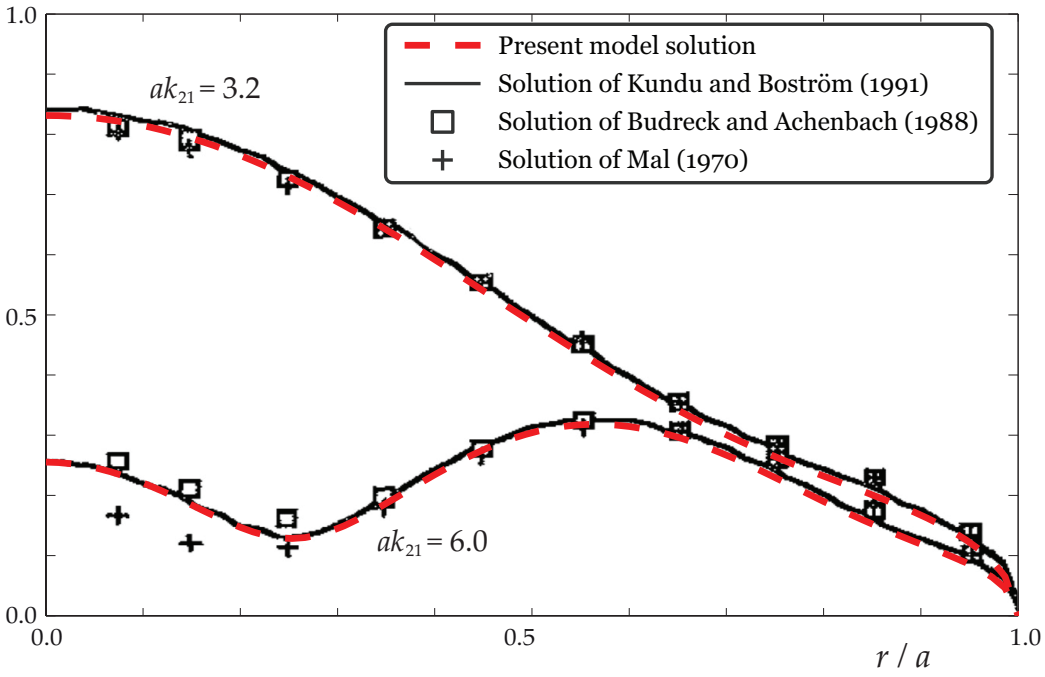

Figure 2: Normalized crack opening displacement for normally incident P wave scattering by a circular crack in a homogeneous medium: comparison with (Mal, 1970; Budreck and Achenbach, 1988; Kundu and Boström, 1991).

where the blocks $\widetilde{\mathbf{A}}^m_{tt'} = \int_0^\infty \mathbf{\Phi}^m_{t'}(\alpha)\widetilde{\mathbf{L}}_{\rm as}(\alpha)\mathbf{\Phi}^m_t(\alpha)\alpha^2\,\mathrm{d}\alpha$ are calculated analytically using the formula

$$\int_0^\infty J_\mu(at)J_\nu(at)\frac{\mathrm{d}t}{t} = \frac{2}{\pi}\frac{\sin(\pi/2(\nu-\mu))}{\nu^2-\mu^2}.$$

In order to check the calculations, a comparison with other papers is performed for the case when the material in the two half-spaces are equal in Fig. 2. The calculations have been performed for glass with parameters given in (Kundu and Boström, 1991). The reasons for the small discrepancies that are seen are unclear, however, note that the results are taken from figures

so that the exact points are a little uncertain. Analogous comparisons have been made for dissimilar media with the method proposed by Glushkov and Glushkova (1996), with a very good correspondence (**?**).

3. Plane wave transmission through a damaged interface

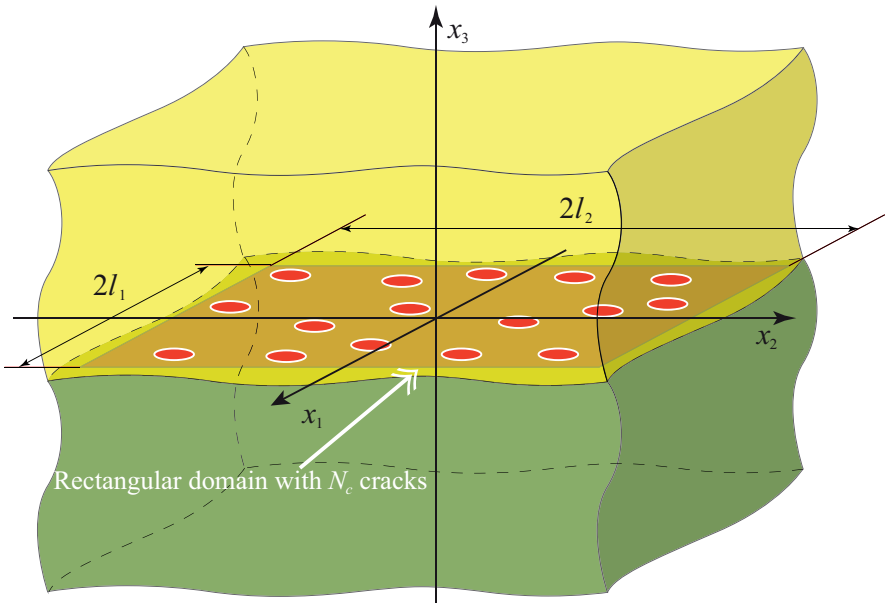

Figure 3: Geometry of the problem for a damaged interface with a distribution of interface cracks.

Following the scheme used in Golub and Boström (2011), consider a plane P or S wave incident normally to an interface with a random distribution of circular cracks of the same radius a, see Fig. 3. It should be mentioned that the scheme can be generalized to the case of cracks with a variation in size. Introduce a large rectangle in the x_1x_2 plane with the center at the origin of coordinates of size $2l_1$ along the x_1 axis and $2l_2$ along the x_2 axis. Then the

crack density parameter C can be introduced as the ratio of the total area of all the cracks S_{damage} to the total area of the rectangle S_{total}

$$C = \frac{S_{damage}}{S_{total}}.$$

The total field is a sum of incident and scattered fields $\boldsymbol{u} = \boldsymbol{u}^{\text{in}} + \boldsymbol{u}^{\text{sc}}$ as for a single crack. The cracks are assumed to be small relative to the wavelength of the incoming wave. It is then possible to neglect the interaction between the cracks if they are not located too close to each other, see more comments later on. The ensemble average of the total scattered field by a random distribution of cracks can be constructed in the same manner as in (Boström and Golub, 2009; Golub and Boström, 2011) in the form of outgoing plane waves propagating in the $\pm x_3$ direction:

$$\langle \boldsymbol{u}^{\text{sc}} \rangle(\mathbf{x}) = \boldsymbol{p}_s \begin{cases} P_s^- \mathrm{e}^{-\mathrm{i}k_{1s}x_3}, & x_3 < 0, \\ P_s^+ \mathrm{e}^{\mathrm{i}k_{2s}x_3}, & x_3 > 0, \end{cases} \tag{16}$$

where the brackets denote ensemble averaging. Here the notation from Section 2 is followed and thus $s = 1$ for the P wave and $s = 2$ for the S wave.

The Betty-Rayleigh reciprocal relation is now applied to the two elastodynamic states $\boldsymbol{u}^{\text{sc}}$ and $\boldsymbol{u}^{\text{in}}$

$$\int_S \left[u_i^{\text{in}}(\mathbf{x}) \cdot \sigma_{ij}^{\text{sc}}(\mathbf{x}) - u_i^{\text{sc}}(\mathbf{x}) \cdot \sigma_{ij}^{\text{in}}(\mathbf{x}) \right] n_j dS = 0.$$

The surface integral is over the area S which is the sum of the rectangular prism S^- with corners at the points $(\pm l_1, \pm l_2, 0^-)$, $(\pm l_1, \pm l_2, -l_3)$ and the rectangular prism S^+ with corners at $((\pm l_1, \pm l_2, 0^+)$, $(\pm l_1, \pm l_2, l_3)$ symmetric to S^- with respect to the x_1x_2 coordinate plane. It can be shown in the same manner as in (Golub and Boström, 2011) that the integrals along the

damaged interface then cancel along the uncracked parts and contain the crack-opening displacement along the cracked parts. Taking an ensemble average the other integrals can all be calculated and this gives for the reflection coefficient

$$P_s^- = -\frac{1}{2}(1 - R_s^-)C\,\boldsymbol{p}_s \cdot \overline{\Delta \boldsymbol{u}}_s,$$

which is expressed in terms of the reflection coefficient R_s^- from equation (4) and the average value of the COD

$$\overline{\Delta \boldsymbol{u}}_s = \frac{1}{\pi a^2} \iint\limits_{\Omega} \Delta \boldsymbol{u}_s(x_1, x_2)\, \mathrm{d}x_1 \mathrm{d}x_2.$$

Here the integration area is over one crack. The transmission coefficient P_s^+ is determined in a similar way (Golub and Boström, 2011):

$$P_s^+ = -\frac{1}{2}(1 + R_s^-)C\boldsymbol{p}_s \cdot \overline{\Delta \boldsymbol{u}}_s.$$

The total transmission coefficient for the random distribution of equal circular cracks then becomes

$$\widetilde{T}_s = T_s^- + P_s^+ = T_s^- \left(1 - \frac{1}{2} C \boldsymbol{p}_s \cdot \overline{\Delta \boldsymbol{u}}_s\right), \tag{17}$$

which is expressed in terms of the material constants, the average of the crack opening displacement and the density of cracks C.

4. Spring boundary conditions

The next step is to transform the calculated transmission coefficient in order to have the same transmission properties as for the spring boundary conditions. If the damaged interface is modelled by the distributed spring model, then spring boundary conditions (1) must be satisfied. The spring

boundary condition (1) demands that normal and tangential stresses $\sigma \cdot \mathbf{n}$ are continuous at the damaged interface, while a displacement jump is proportional to the stresses. The diagonal components of the three-by-three matrix $\boldsymbol{\kappa}$ are determined below from equality of the transmission coefficients for the random distribution of cracks and the spring model. As in Section 2, the displacement field for both types of plane waves ($s = 1, 2$) normally incident to the interface $x_3 = 0$ and incoming from the lower half-space ($x_3 < 0$) is

$$\boldsymbol{u}_s(\mathbf{x}) = \begin{cases} \boldsymbol{p}_s \left(\mathrm{e}^{\mathrm{i}k_{1s}x_3} + \widehat{R}_s \mathrm{e}^{-\mathrm{i}k_{1s}x_3} \right), & x_3 < 0, \\ \boldsymbol{p}_s \widehat{T}_s \mathrm{e}^{\mathrm{i}k_{2s}x_3}, & x_3 > 0, \end{cases} \tag{18}$$

$$\widehat{R}_s = \frac{\mathrm{i}c_{1s}k_{1s}c_{2s}k_{2s} + \kappa_s(c_{1s}k_{1s} - c_{2s}k_{2s})}{\mathrm{i}c_{1s}k_{1s}c_{2s}k_{2s} + \kappa_s(c_{1s}k_{1s} + c_{2s}k_{2s})},$$

$$\widehat{T}_s = \frac{2\kappa_s c_{1s}k_{1s}}{\mathrm{i}c_{1s}k_{1s}c_{2s}k_{2s} + \kappa_s(c_{1s}k_{1s} + c_{2s}k_{2s})}. \tag{19}$$

In the limit $\kappa_s \to \infty$ these reflection and transmission coefficient becomes identical to those in Section 2 for a welded interface.

The spring model assumes that it gives the same transmission as a random distribution of interface cracks. So the transmission coefficients (19) and (17) for the distributed spring model and the random distribution are set equal: $\widetilde{T}_s = \widehat{T}_s$ and this gives

$$\kappa_N = \kappa_{33} = f_1 \left(\frac{1}{C\,\boldsymbol{p}_1 \cdot \overline{\Delta \boldsymbol{v}}_1} - \frac{1}{2} \right), \quad \kappa_T = \kappa_{11} = f_2 \left(\frac{1}{C\,\boldsymbol{p}_2 \cdot \overline{\Delta \boldsymbol{v}}_2} - \frac{1}{2} \right). \tag{20}$$

$$f_s = \frac{2\mathrm{i}c_{1s}k_{1s}c_{2s}k_{2s}}{c_{1s}k_{1s} + c_{2s}k_{2s}}.$$

The second terms in the estimations (20) depend on frequency, so from the assumptions of $ak_{nj} \ll 1$ these terms can be omitted.

In the relation (20) the average crack opening displacement $\overline{\Delta \boldsymbol{u}_s}$ is needed to determine the normal and transverse spring stiffnesses $\kappa_{33} = \kappa_N$ and $\kappa_{11} = \kappa_{22} = \kappa_T$. Instead of a numerical calculation of $\Delta \boldsymbol{u}_s$, an asymptotic solution $\Delta \boldsymbol{u}_s^{\mathrm{as}}$ can be used in (20). Construction of the asymptotic solution $\Delta \boldsymbol{u}_s^{\mathrm{as}}$ is based on the assumption that $ak_{nj} \ll 1$. This assumption makes it possible to exploit the expansions (13) for γ_{nj} again, so the integrals in the left-hand side of system of algebraic equations can be estimated as $\mathbf{A}_{tt'}^m \approx \widetilde{\mathbf{A}}_{tt'}^m$, because

$$\int_0^\infty \boldsymbol{\Phi}_{t'}^m(\alpha) \widetilde{\mathbf{L}}(\alpha) \boldsymbol{\Phi}_t^m(\alpha) \, \mathrm{d}\alpha \to 0$$

as $ak_{nj} \to 0$. In the system of equations (12) the matrix $\mathbf{A}_{tt'}^m \approx \widetilde{\mathbf{A}}_{tt'}^m$ is thus known in closed form. For P wave incidence only $m = 0$ and $n = 0$ enter and it is enough to put the number of terms in the COD expansion $N_t = 0$ because the coefficients $|\boldsymbol{\beta}_t^{10}|$ decay rapidly with t when $ak_{nj} \ll 1$. If only the first term is kept in the expansion (10), then the asymptotic solution for the COD can be obtained analytically by solving a three-by-three system of linear algebraic equations $\widetilde{\mathbf{A}}_{00}^0 \widehat{\boldsymbol{\beta}}_0^{10} = \boldsymbol{g}_{01}^{10}$:

$$\widehat{\beta}_{10}^{\mathrm{as},10} = f_1 \frac{20am_3(m_1^2 - m_3^2)}{4\pi^2 m_1^2 - 15m_3^2},$$

$$\widehat{\beta}_{20}^{\mathrm{as},10} = f_1 \frac{20am_3(m_1^2 - m_3^2)}{4\pi^2 m_1^2 - 15m_3^2},$$

$$\widehat{\beta}_{30}^{\mathrm{as},10} = f_1 \frac{8a\pi m_1(m_1^2 - m_3^2)}{4\pi^2 m_1^2 - 15m_3^2}.$$

The systems of linear algebraic equations (12) should also be solved for SV wave incidence, the non-zero terms are then for $m = 1$ and $n = 1$. The coefficients $\widehat{\beta}_{k0}^{11}$ are more complex as compared to P-wave incidence :

$$\widehat{\beta}_{10}^{\mathrm{as},11} = f_2 \frac{1680am_2^2 m_3^2(m_1^2 - m_3^2)}{\pi(m_1^2 + m_1m_2 - m_3^2)(36m_1\pi^2(m_1^2 + m_1m_2 - m_3^2) - 275m_2m_3^2)},$$

$$\widehat{\beta}_{20}^{\mathrm{as},11} = f_2 \frac{-32am2(m_1^2 - m_3^2)(9m_1\pi^2(m_1^2 + m_1m_2 - m_3^2) - 35m_2m_3^2)}{\pi(m_1^2 + m_1m_2 - m_3^2)(36m_1\pi^2(m_1^2 + m_1m_2 - m_3^2) - 275m_2m_3^2)},$$

$$\widehat{\beta}_{30}^{\mathrm{as},11} = f_2 \frac{-360a\pi m_2m_3(m_1^2 - m_3^2)}{\pi(36m_1\pi^2(m_1^2 + m_1m_2 - m_3^2) - 275m_2m_3^2)}.$$

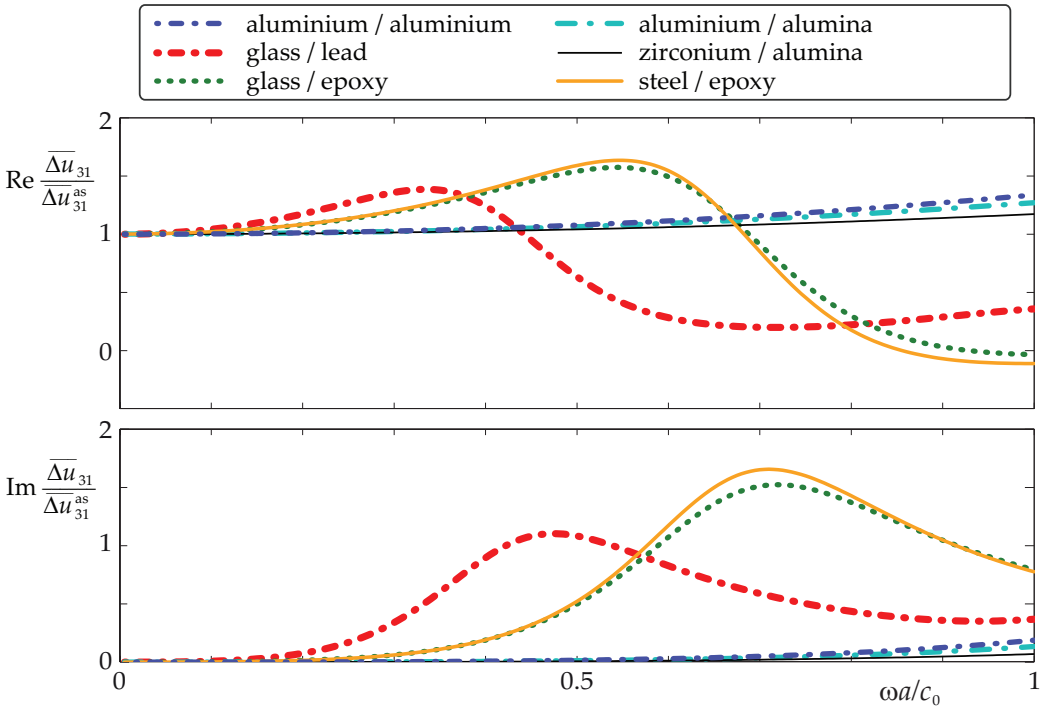

Figure 4: The averaged vertical COD $\overline{\Delta u}_{31}$ obtained numerically divided by the averaged asymptotic solution $\overline{\Delta u}_{31}^{\mathrm{as}}$ for P wave diffraction by a single interface crack between six different combinations of media at $N_t = 10$; $c_0 = 3160$m/s.

In order to demonstrate the accuracy of the asymptotic solution, Fig. 4 shows the averaged vertical COD component $\overline{\Delta u}_{31}$ divided by the purely real average $\overline{\Delta u}_{31}^{\mathrm{as}}$ of asymptotic solution $\Delta u_{31}^{\mathrm{as}}(r,\theta) = \beta_{30}^{\mathrm{as},10}\phi_{30}^{10}(r)$ for six pairs of materials (their properties are listed in Table 1). Fig. 4 depicts the real and imaginary parts for $N_t = 10$, and as there are only small changes going from

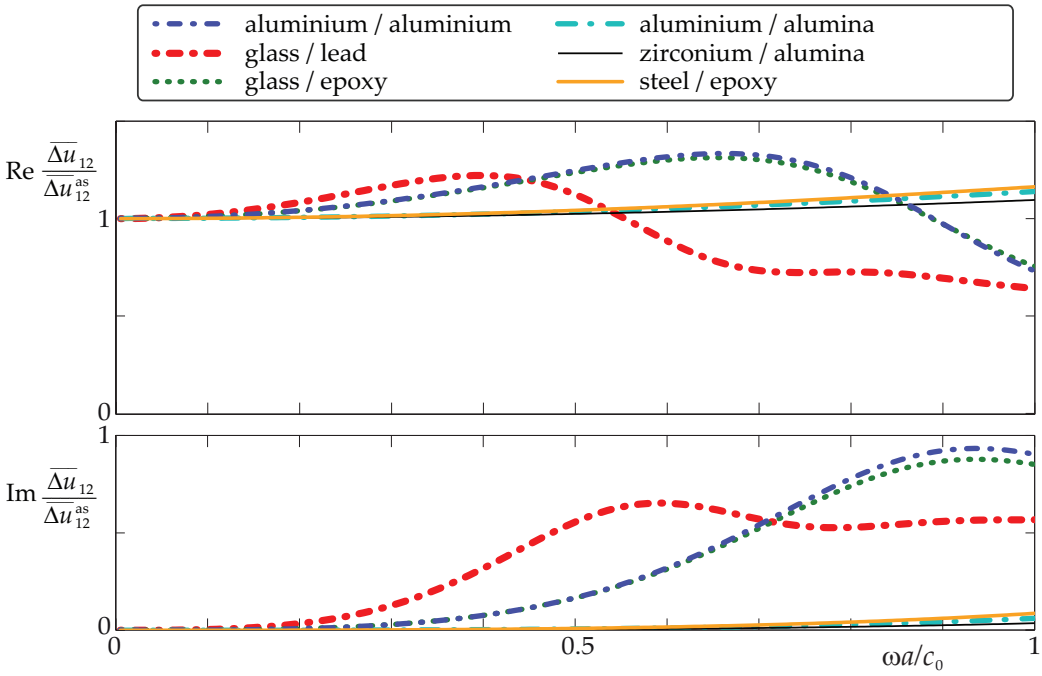

Figure 5: The averaged horizontal COD $\overline{\Delta u}_{12}$ obtained numerically divided by the averaged asymptotic solution $\overline{\Delta u}^{as}_{12}$ for SV-wave diffraction by a single interface crack between six different combinations of media at $N_t = 10$.

$N_t = 0$ to $N_t = 10$ it is concluded that the asymptotic solution is accurate enough for the estimation of the normal spring stiffness. The relative error is less than 1% when $ak \lesssim 0.2$. The same comparison of $\overline{\Delta u}_{12}$ and $\overline{\Delta u}^{as}_{12}$ is demonstrated in Fig. 5 for SV-wave scattering.

Using the asymptotic solutions mentioned above, the transverse and normal spring stiffnesses are obtained as:

$$\kappa_i = \kappa_i^0 \cdot \frac{1}{aC}, \quad i = T, N, \tag{21}$$

Material	Density, ρ [kg/m^3]	Young's modulus, E [GPa]	Poison ratio, ν
Glass	2770	69.15	0.25
Alumina	4000	400	0.231
Epoxy	1200	4.5	0.399
Aluminium	2700	70	0.33
Zirconium	5700	200	0.3
Lead	11400	17.76	0.43
Steel	7860	81	0.288

Table 1: Dimensionless mass densities and wave velocities of the materials used.

where

$$\kappa_N^0 = \frac{3}{16\pi} \cdot \frac{15m_3^2 - 4\pi m_1^2}{m_1(m_1^2 - m_3^2)},$$

$$\kappa_T^0 = \frac{3\pi(m_1^2 + m_1 m_2 - m_3^2)}{32 m_2(m_1^2 - m_3^2)} \cdot \frac{36 m_1 \pi^2 (m_1^2 + m_1 m_2 - m_3^2) - 275 m_2 m_3^2}{9 m_1 \pi^2 (m_1^2 + m_1 m_2 - m_3^2) - 35 m_2 m_3^2}.$$

The obtained formulae (21) are now compared with the stiffnesses derived for a periodic hexagonal array of circular cracks by Lekesiz et al. (2013a), who estimated the normal and transverse spring stiffnesses based on the methods of Lekesiz et al. (2013b) and Kachanov (1994). In the case considered by (Lekesiz et al., 2013a) distance between neighbour circular cracks of radius a is equal $2b$, so the corresponding unit-cell including one crack has side $2\sqrt{3}b/3$. The crack density is then calculated as the ratio of the area of the circular crack πa^2 and the area of the hexagonal unit cell

$$C = \frac{\pi a^2}{2\sqrt{3}b^2}.$$

Thus, stiffnesses (21) can be rewritten in the following form

$$\kappa_i \cdot b = \kappa_i^0 \cdot I\left(a/b\right), \quad i = T, N, \tag{22}$$
$$I\left(\frac{a}{b}\right) = \frac{3\sqrt{3}}{2} \cdot \left(\frac{a}{b}\right)^{-3}.$$

The stiffnesses derived in Lekesiz et al. (2013a) have similar form

$$\kappa_{i,\text{Lekesiz}} \cdot b = \kappa_{i,\text{Lekesiz}}^0 \cdot I_{\text{Lekesiz}}\left(a/b\right), \quad i = T, N, \tag{23}$$

which are expressed in terms of the function

$$I_{\text{Lekesiz}}\left(\frac{a}{b}\right) = \frac{\pi^2 D_{\text{L}}}{8} \cdot \frac{3\pi}{4} \cdot \left(\frac{a}{b}\right)^{\frac{1}{2}} \cdot \left[\ln \sec\left(\frac{\pi\sqrt{D_{\text{L}}}}{2}\left(\frac{a}{b}\right)^{\frac{7}{4}}\right)\right]^{-1},$$

where $D_{\text{L}} = 0.8673$ and $\kappa_{i,\text{Lekesiz}}^0$ are given in Lekesiz et al. (2013a).

The case of identical materials is considered first in order to have a clear analytical comparison of the estimations obtained in (Lekesiz et al., 2013a) and derived via the present approach. The effective transverse and normal spring stiffnesses for identical materials are given by (Lekesiz et al., 2013a, Eqs. (25) and (26)) in terms of elastic moduli $\lambda = \lambda_1 = \lambda_2$ and $\mu = \mu_1 = \mu_2$, crack radius a and average distance between defects $2b$:

$$\begin{aligned}
\kappa_{T,\text{Lekesiz}}^{\text{homogeneous}} \cdot b &= \frac{\mu(3\lambda + 4\mu)}{4(\lambda + 2\mu)} \cdot I_{\text{Lekesiz}}\left(\frac{a}{b}\right), \\
\kappa_{N,\text{Lekesiz}}^{\text{homogeneous}} \cdot b &= \frac{\mu(\lambda + \mu)}{\lambda + 2\mu} \cdot I_{\text{Lekesiz}}\left(\frac{a}{b}\right).
\end{aligned} \tag{24}$$

The present stiffnesses given by the relations (21) are simplified in the case of identical materials (taking into account that $m_3 = 0$) and expressed in terms of a and b (instead of C):

$$\begin{aligned}
\kappa_T^{\text{homogeneous}} \cdot b &= \frac{\mu(3\lambda + 4\mu)}{4(\lambda + 2\mu)} \cdot I\left(\frac{a}{b}\right), \\
\kappa_N^{\text{homogeneous}} \cdot b &= \frac{\mu(\lambda + \mu)}{\lambda + 2\mu} \cdot I\left(\frac{a}{b}\right).
\end{aligned} \tag{25}$$

The dependencies on the Lamé parameters are the same for the normal and tangential stiffnesses in the case of identical materials. Moreover, the dependencies on the Lamé parameters are in a very good agreement ($\kappa_i^0 \approx \kappa_{i,\text{Lekesiz}}^0$) also for dissimilar materials as demonstrated in Table 2.

	$\kappa_T^0/\kappa_{T,\text{Lekesiz}}^0$	$\kappa_N^0/\kappa_{N,\text{Lekesiz}}^0$
aluminium / aluminium	1.0	1.0
glass / lead	1.00002	1.00003
glass / epoxy	1.00062	1.00102
aluminium / alumina	1.00084	1.00147
zirconium / alumina	1.00015	1.00026
steel / epoxy	1.00086	1.00143

Table 2: Ratios $\kappa_T^0/\kappa_{T,\text{Lekesiz}}^0$ and $\kappa_N^0/\kappa_{N,\text{Lekesiz}}^0$ for different pairs of materials.

The dependence on a/b seems very different at first glance, but as shown in Fig. 6 the difference is small for small a/b and then gradually increases. To capture the relative difference it is better to consider the ratio $\kappa_i/\kappa_{i,\text{Lekesiz}}$, very nearly coinciding with $I(a/b)/I_{\text{Lekesiz}}(a/b)$ due to the approximate equality of the multipliers depending on elastic moduli. Figure 7 depicts the spring stiffnesses calculated via formulae (21) normalized by the corresponding stiffnesses from (Lekesiz et al., 2013a, Eqs. (40) and (41)) valid for identical and dissimilar media. For small a/b it can be seen that the spring stiffnesses are about 10.3% greater as compared to the hexagonal array of periodic cracks. One reason for this difference is the difference between a periodic and a stochastic crack distribution. Thus, the transmission coefficient for periodic

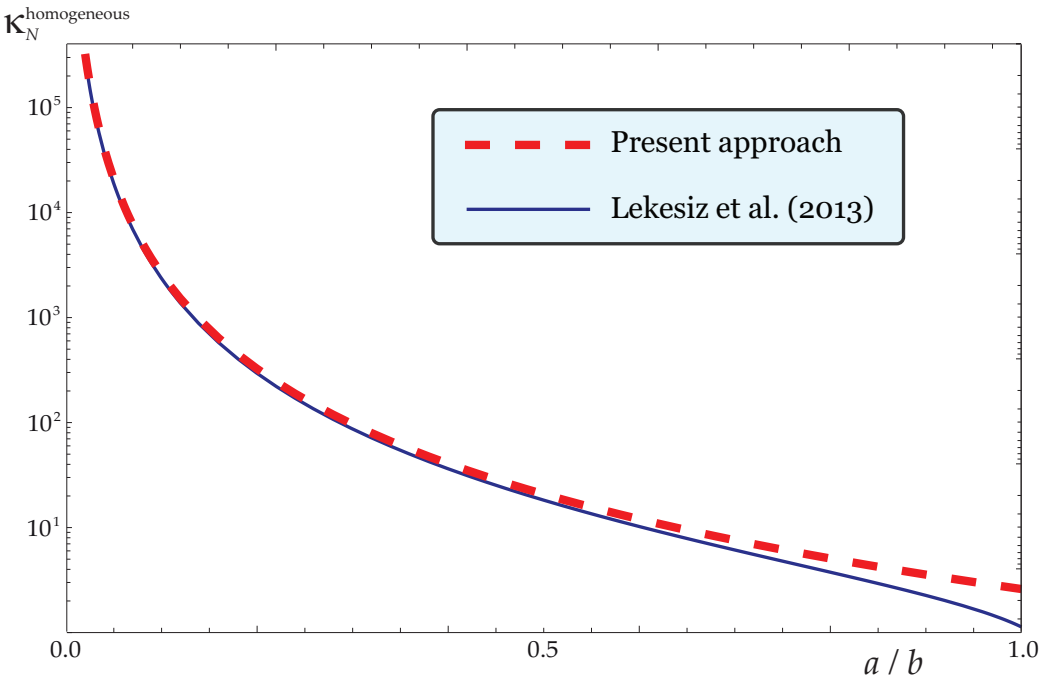

Figure 6: Normal spring stiffnesses $\kappa_N^{\text{homogeneous}}(a/b)$ obtained in the present work and $\kappa_{N,\text{Lekesiz}}^{\text{homogeneous}}(a/b)$ derived in (Lekesiz et al., 2013a) for identical materials normalized with $b(\lambda_2 + 2\mu_2)/\mu_2(\lambda_2 + \mu_2)$.

strip-like cracks and the spring model was considered by Golub and Boström (2011). It was demonstrated that the transmission is about 10% greater for the spring model based on the assumption of a stochastic distribution of cracks compared to an periodic array of cracks. A very similar conclusion was made by (Sotiropoulos and Achenbach, 1988, Eq. (46)), who demonstrated that periodic circular cracks have approximately 11% lower reflection coefficient than the statistical distributions of circular cracks.

For high crack densities the present approach deviates more and more from the results for periodic cracks. This is mainly due to the neglect of

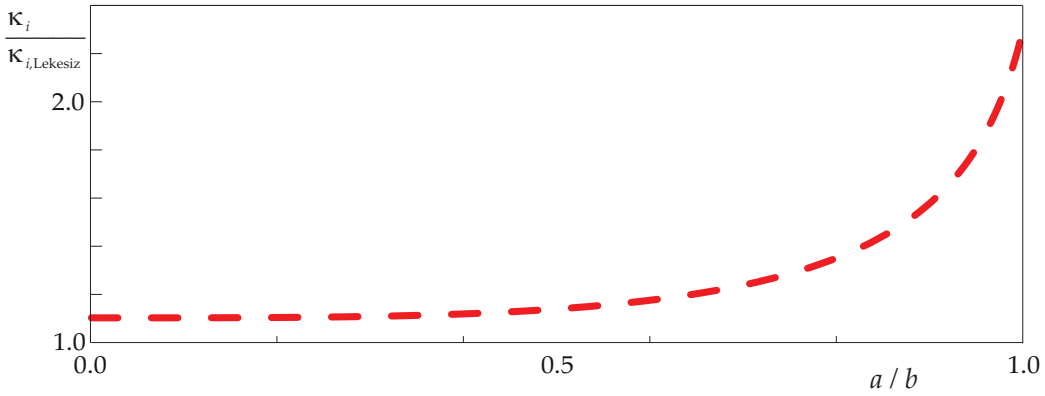

Figure 7: Ratio between spring stiffnesses $\kappa_i(a/b)$ obtained in the present work and $\kappa_{i,\text{Lekesiz}}(a/b)$ derived in (Lekesiz et al., 2013a) approximately valid for arbitrary pairs of materials.

multiple scattering in the present approach, but maybe also because the stochastic distribution tends to loose it meaning when the crack density becomes large. It has been shown by Isida et al. (1985) that the static interaction effects between two coplanar elliptical cracks are negligible if distances between crack centers s and crack diameters d satisfy the relation

$$s/d \gtrsim 1.25,$$

which transforms for hexagonal periodic cracks ($s = 2b$ and $d = 2a$) into

$$a/b \lesssim 0.8$$

But as shown by (Sotiropoulos and Achenbach, 1988, Eq. (46)) the neglect of multiple scattering is valid for surprisingly large crack densities at low frequencies. Thus, it could be quantified so that multiple scattering is neglected with good accuracy at least for $a/b \lesssim 0.5$ ($C \lesssim 0.23$).

5. Concluding remarks

Spring boundary conditions for simulation of damaged interfaces are derived in a three-dimensional case. The normal and transverse effective spring stiffnesses are expressed in terms of elastic moduli, damage parameters and frequency. The stiffnesses have been derived for small sizes of cracks compared to the wavelength and stochastically distributed microcracks, so the results differ from the stiffnesses of Lekesiz et al. (2013a) derived for periodic cracks. The model should be valid when the crack radius a fulfills $\max ka \lesssim 0.2$, where max is with respect to all the wave numbers k in the two media, and when the damage parameter $a/b \lesssim 0.5$ ($C \lesssim 0.23$). The spring boundary conditions can be applied for different kinds of problems, e.g. by measuring the group velocity to find a damaged part of an interface (Balvantin et al., 2012; Mezil et al., 2014) or by using wave velocities from local maximum and minimum frequencies of the reflection spectrum to obtain a normal interfacial stiffnesses for multilayered structures (Ishii and Biwa, 2014).

6. Acknowledgments

The joint research became possible thanks the Swedish Institute. The authors are grateful to Professors E.V. Glushkov and N.V. Glushkova for valuable discussions. The work is supported by the Ministry of Education and Science of the Russian Federation (Project 1.189.2014K).

References

Achenbach, J.D., 1989. Effects of crack geometry and material behavior on scattering by cracks. Technical Report. Center for Quality Engineering and Failure Prevention Northwestern University.

Achenbach, J.D., Zhang, C., 1990. Reflection and transmission of ultrasound by a region of damaged material. Journal of Nondestructive Evaluation 9, 22–32.

Alers, G., Graham, L., 1975. Reflection of ultrasonic waves by thin interfaces, in: Ultrasonics Symposium, pp. 579–582. doi:10.1109/ULTSYM.1975.196590.

Baik, J.M., Thompson, R.B., 1984. Ultrasonic scattering from imperfect interfaces: a quasi-static model. Journal of Nondestructive Evaluation 4, 177–196.

Balvantin, A., Baltazar, A., Aranda-Sanchez, J.I., 2012. A study of guided wave propagation on a plate between two solid bodies with imperfect boundary conditions. International Journal of Mechanical Sciences 63, 66 – 73. doi:http://dx.doi.org/10.1016/j.ijmecsci.2012.06.013.

Boström, A., Golub, M.V., 2009. Elastic SH wave propagation in a layered anisotropic plate with interface damage modelled by spring boundary conditions. Quarterly Journal of Mechanics and Applied Mathematics 62, 39–52.

Boström, A., Peterson, L., 1989. Wave scattering by a circular crack in the interface between two elastic media. Technical Report. Report 1989:7,

Division of Mechanics, Chalmers University of Technology, Goteburg, Sweden.

Boström, A., Wickham, G.R., 1991. On the boundary conditions for ultrasonic transmission by partially closed cracks. Journal of Nondestructive Evaluation 10, 139–149.

Budreck, D., Achenbach, J.D., 1988. Scattering from three-dimensional planar cracks by the boundary integral equation method. Journal of Applied Mechanics 55, 405–412. doi:10.1115/1.3173690.

Glushkov, E.V., Glushkova, N.V., 2001. On the efficient implementation of the integral equation method in elastodynamics. Journal of Computational Acoustics 9(3), 889–898.

Glushkov, E.V., Glushkova, N.V., Ekhlakov, A.V., 2002. A mathematical model of the ultrasonic detection of three-dimensional cracks. Journal of Applied Mathematics and Mechanics 66, 141 – 149.

Glushkov, Ye.V., Glushkova, N.V., 1996. Diffraction of elastic waves by three-dimensional cracks of arbitrary shape in a plane. Journal of Applied Mathematics and Mechanics 60, 277–283.

Golub, M.V., 2010. Propagation of elastic waves in layered composites with microdefect concentration zones and their simulation with spring boundary conditions. Acoustical Physics 56(6), 848–855.

Golub, M.V., Boström, A., 2011. Interface damage modelled by spring boundary conditions for in-plane elastic waves. Wave Motion 48(2), 105–115. doi:10.1016/j.wavemoti.2010.09.003.

Ishii, Y., Biwa, S., 2014. Evaluation of interlayer interfacial stiffness and layer wave velocity of multilayered structures by ultrasonic spectroscopy. Journal of the Acoustical Society of America 136, 183191. doi:http://dx.doi.org/10.1121/1.4881920.

Isida, M., Hirota, K., Noguchi, H., Yoshida, T., 1985. Two parallel elliptical cracks in an infinite solid subjected to tension. International Journal of Fracture 27, 31–48. doi:10.1007/BF00017211.

Kachanov, M., 1994. Elastic solids with many cracks and related problems. Advances of Applied Mechanics 30, 259445.

Krenk, S., Schmidt, H., 1982. Elastic wave scattering by a circular crack. Philosophical Transactions of the Royal Society of London. Series A, Mathematical and Physical Sciences 308, 167–198.

Kundu, T., Boström, A., 1991. Elastic wave scattering by a circular crack in a transversely isotropic solid. Journal of Applied Mechanics. Transactions of the ASME 58, 695–702.

Kvasha, O., Boström, A., Glushkova, N., Glushkov, E., 2011. The propagation of in-plane p-sv waves in a layered elastic plate with periodic interface cracks: exact versus spring boundary conditions. Waves in Random and Complex Media 21, 515–528. doi:10.1080/17455030.2011.593586.

Lavrentyev, A.I., Rokhlin, S.I., 1994. Models for ultrasonic characterization of environmental degradation of interfaces in adhesive joints. Journal of Applied Physics 76, 4643–4650.

Lavrentyev, A.I., Rokhlin, S.I., 1998. Ultrasonic spectroscopy of imperfect contact interfaces between a layer and two solids. Journal of the Acoustical Society of America 103, 657–664.

Leiderman, R., Castello, D., 2014. Scattering of ultrasonic waves by heterogeneous interfaces: Formulating the direct scattering problem as a least-squares problem. The Journal of the Acoustical Society of America 135, 5–16. doi:http://dx.doi.org/10.1121/1.4845615.

Lekesiz, H., Katsube, N., Rokhlin, S., Seghi, R.R., 2013a. Effective spring stiffness for a periodic array of interacting coplanar penny-shaped cracks at an interface between two dissimilar isotropic materials. International Journal of Solids and Structures 50, 2817 – 2828. doi:http://dx.doi.org/10.1016/j.ijsolstr.2013.04.006.

Lekesiz, H., Katsube, N., Rokhlin, S., Seghi, R.R., 2013b. The stress intensity factors for a periodic array of interacting coplanar penny-shaped cracks. International Journal of Solids and Structures 50, 186 – 200. doi:http://dx.doi.org/10.1016/j.ijsolstr.2012.09.018.

Lekesiz, H., Katsube, N., Rokhlin, S.I., Seghi, R.R., 2011. Effective spring stiffness for a planar periodic array of collinear cracks at an interface between two dissimilar isotropic materials. Mechanics of Materials 43, 87–98.

Mal, A., 1970. Interaction of elastic waves with a penny-shaped crack. International Journal of Engineering Science 8, 381–388.

Margetan, F.J., Thompson, R.B., Gray, T.A., 1988. Interfacial spring model for ultrasonic interactions with imperfect interfaces: Theory of oblique

incidence and application to diffusion-bonded butt joints. Journal of Nondestructive Evaluation 7, 131–152.

Mezil, S., Laurent, J., Royer, D., Prada, C., 2014. Non contact probing of interfacial stiffnesses between two plates by zero-group velocity lamb modes. Applied Physics Letters 105, 021605. doi:http://dx.doi.org/10.1063/1.4890110.

Ohyoshi, T., 1973. Effect of orthotropy on singular stress produced near a crack tip by incident SH waves. ZAMM - Journal of Applied Mathematics and Mechanics / Zeitschrift für Angewandte Mathematik und Mechanik 53, 409–411.

Pecorari, C., 2008. Spring boundary model for a partially closed crack. International Journal of Engineering Science 46, 182–188.

Shifrin, E., 2015. Inverse spectral problem for a rod with multiple cracks. Mechanical Systems and Signal Processing 5657, 181 – 196. doi:http://dx.doi.org/10.1016/j.ymssp.2014.11.004.

Sotiropoulos, D.A., Achenbach, J.D., 1988. Ultrasonic reflection by a planar distribution of cracks. Journal of Nondestructive Evaluation 7, 123–129.

Srivastava, K.N., Palaiya, R.M., Gupta, O.P., 1979. Interaction of longitudinal wave with a penny-shaped crack at the interface of two bonded dissimilar elastic solids-ii. International Journal of Fracture 15, 591–599.

Tattersall, H.G., 1973. The ultrasonic pulse-echo technique as applied to adhesion testing. Journal of Physics D: Applied Physics 6, 819–832. doi:10.1088/0022-3727/6/7/305.

Vatulyan, A., Yavruyan, O., 2006. An asymptotic approach in problems of crack identification. Journal of Applied Mathematics and Mechanics 70, 647 – 656. doi:http://dx.doi.org/10.1016/j.jappmathmech.2006.09.015.